UDC 620.18:669.14.018.44:621.172.251.2

STRUCTURAL CHANGES IN REFRACTORY STEEL 10Kh9V2MFBR DUE TO CREEP AT 650°C

V. A. Dudko,[1] A. N. Belyakov,[1] V. N. Skorobogatykh,[2] I. A. Shchenkova,[2] and R. O. Kaibyshev[1]

Changes in the structure of steel 10Kh9V2MFBR after creep tests are studied. It is shown that annealing causes inconsiderable changes in the structure of troostomartensite formed due to tempering in the head of a specimen. In the functional part of the specimen, on the contrary, the place of the initial troostomartensite is taken by coarse equiaxed subgrains; the density of the lattice dislocations decreases by an order of magnitude. The change in the microstructure in the process of creep causes a more than 30% decrease in the hardness of the material.

Keywords: refractory steel, structure, creep, off-orientation of grain/subgrain boundaries.

INTRODUCTION

Today, martensitic steels with 9 – 12% Cr are treated as promising refractory materials for coal-fired thermal power plants [1 – 3]. The creep resistance of these materials at elevated temperatures is ensured by the structure formed as a result of normalizing and tempering [4]. A high creep resistance is attained due to two factors. Firstly, the carbonitrides of type Me(C, N) and the carbides of type $Me_{23}C_6$ have a size of less than 50 and 100 μm, respectively, which ensures effective precipitation hardening [4, 10]. Secondly, these particles ensure stability of the dislocation structure of the troostomartensite in creep [4 – 9], which is an additional factor raising the creep resistance of steels of martensitic class. The first condition for high creep resistance of these steels is the resistance of the carbides to coagulation, because these carbides, in addition to the tungsten and molybdenum dissolved in the ferrite matrix, promote stabilization of the dislocation structure of the troostomartensite [3 – 6]. The long-term stability of the tempered martensite structure, caused by the invariability of the size and specific volume of the fine particles in the creep process, controls the creep resistance of these steels and determines the ultimate long-term strength and the time before failure. From this standpoint a general approach to improving the chemical and phase composition of steels of martensitic class aimed at raising their creep resistance consists in raising the stability of the structure of the troostomartensite. In order to implement this approach we should possess detailed information on the regular features of the evolution of microstructure in these materials, on the mechanisms of coagulation of the carbides, and on the segregation and growth of Laves phases in the process of creep. Unfortunately, works devoted to this problem are relatively few [4 – 9].

The aim of the present work consisted in studying the structural changes simultaneously in the functional part of a specimen of steel 10Kh9V2MFBR and in its undeformed part in the process of creep at a temperature of 650°C, which is somewhat higher than the operating temperature (620°C) of this steel. This makes it possible to differentiate between the structural changes in the steel due to annealing and the microstructural changes connected with the creep.

METHODS OF STUDY

We studied specimens with diameter of 10 mm and a functional part 50 mm long, which had been cut from hot-deformed tubes from steel 19Kh9V2MFBR (0.1% Cr, 0.17% Si, 0.54% Mn, 8.75% Cr, 0.21% Ni, 0.51% Mo, 1.60% W, 0.23% V, 0.07% Nb, remainder Fe) produced at the Chelyabinsk Tube-Rolling Plant. The tubes were subjected to normalizing from 1050°C and tempering at 720°C for 3 h. The creep tests were continued until failure at 650°C at a stress of 118 MPa using a lever-type machine. The microstructure was studied on a specimen that had failed after 1271 h. We analyzed the structural changes in the head and in the neck of the specimen after testing it for creep. The data obtained were compared with the initial structure formed after the tempering.

[1] Belgorod State University, Belgorod, Russia (E-mail: dudko@bsu.edu.ru, rustam kaibyshev@bsu.edu.ru).

[2] Central Research Institute for Machine-Building Technology (GNTs RF OAO NPO "TsNIITMASh"), Moscow, Russia.

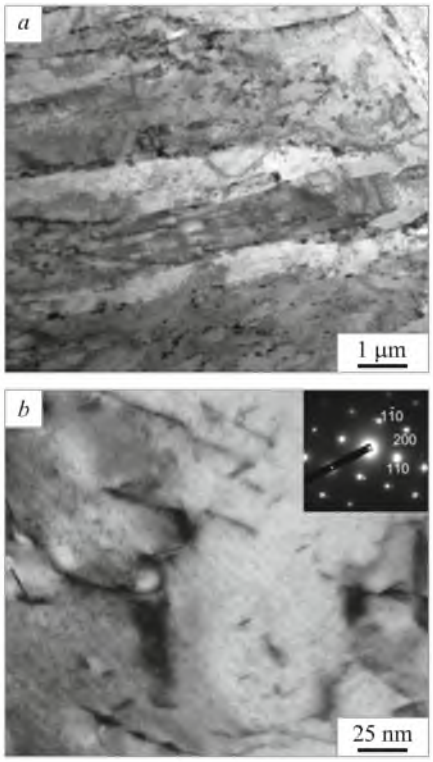

Fig. 1. Tempered martensite in refractory steel 10Kh9V2MFBR: *a*) comparatively large segregations of secondary phases on boundaries of blocks and laths; *b*) fine carbides inside laths.

The structure of the specimens was studied with the help of a Quanta 600 scanning electron microscope equipped with an attachment for analyzing off-orientations by the EBSD method. The maps of the off-orientations were corrected at a minimum parameter of certainty equal to 0.1. The fine structure was studied using a Jeol JEM-2100 transmission electron microscope (TEM) with an attachment for energy dispersive analysis. The sizes of the subgrains were measured by the method of secants using TEM photographs. We took into account all the subgrains with well-discernible subboundaries. The dislocation density was determined by calculating individual dislocations in internal regions of grains/subgrains, for at least six randomly chosen characteristic TEM photographs of each specimen. The foils for the TEM were fabricated by the method of jet electrochemical polishing using a 10% solution of perchloric acid in acetic acid and a Struers TenuPol-5 device. The microhardness was measured with the help of a Wolpert 402MVD digital microhardness meter at a load of 5 N in the central part over the axis of the specimen from the region of the head to the region of the neck.

RESULTS

Microstructure after Tempering

A typical fine structure of steel 10Kh9V2MFBR is presented in Fig. 1*a*. The size of the initial austenite grains was about 20 μm. It can be seen that this is a typical structure of packet martensite consisting of several packets inside former austenite grains. Every packet contains blocks divided into laths by primarily small-angle boundaries. The transverse size of the laths is about 330 nm. The dislocation density is quite high, i.e., $\rho = 6.2 \times 10^{14}$ m^{-2}. The boundaries of the packets and blocks are decorated with segregations of secondary phases, primaliry $Me_{23}C_6$, with a mean size of about 85 nm and a volume fraction of about 2%. Lamellar particles of V(C, N) are uniformly distributed inside the laths (Fig. 1*b*). The crystallographic orientation of the particles with respect to the matrix meets the orientation relation of Baker – Nutting [9], i.e., $(100)_{V(C,N)} \parallel (100)_{\alpha}$, $[011]_{V(C,N)} \parallel [001]_{\alpha}$. The mean longitudinal size and the thickness of these fine carbonitrides is 8 and 2 nm, respectively, and the number of particles per unit volume $N_V = 2 \times 10^{22}$ m^{-3}, i.e., their volume fraction is about 0.02%. The mean distance between the carbonitrides was calculated under the assumption that the V(C, N) nanoparticles were distributed over the sites of a square lattice [11]. It turned out to be equal to about 100 nm.

A specific bimodal distribution of boundaries over the off-orientation angles arises as a result of the martensitic transformation (Fig. 2). The plot exhibits two well manifested peaks at $\theta = 10$ and 60°. The small-angle off-orientations correspond to the small-angle boundaries of the laths having a dislocation nature, whereas the large-angle off-orientations are chiefly connected with block boundaries, the majority of which are special $\Sigma 3$ boundaries whose specific fraction in the structure of the tempered martensite is about 9%. It should be noted that special boundaries dividing the blocks into laths are encountered rarely.

Softening of the Steel during Creep

The microhardness of tempered steel 10Kh9V2MFBR is 268 *HV*. After the creep tests it decreases considerably. However, the softening over the length of the specimen is nonuniform. In order to study the effect of plastic deformation on the softening we measured the microhardness in the central part of the specimen over the axis from the head to the neck at a step of about 2 mm, as shown in Fig. 3. In this figure we also present the contraction measured in the same sections as the microhardness. The microhardness decreases progressively from 234 *HV* at a place near the head to 182 *HV* in the neck of the specimen. It can be seen from Fig. 3 that the decrease in the microhardness due to creep correlates with the degree of plastic deformation. The microhardness drops to 210 *HV* in that part of the specimen that has experienced uniform deformation (5% contraction). Localization of plastic yielding in the neck decreases the microhardness to 182 *HV*, i.e., annealing at he test temperature results in 12% decrease in the microhardness, whereas the change in the microstructure of the deformed part decreases it by 32%. In other words, the considerable softening of the steel is directly con-

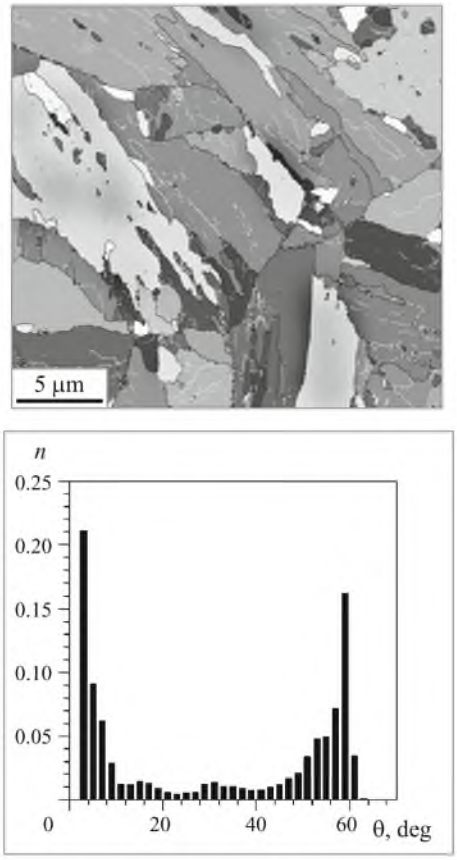

Fig. 2. Maps of off-orientation and distribution of grain/subgrain boundaries with respect to the off-orientation angles (n is the numerical fraction of the boundaries and θ is the off-orientation angle) in tempered martensite of refractory steel 10Kh9V2MFBR. The boundaries with off-orientation of less than and greater than 15° are shown white and black respectively.

nected with plastic deformation. Let us consider the structural changes in the test process in greater detail.

MICROSTRUCTURE OF THE STEEL AFTER ANNEALING AND CREEP

The maps of off-orientations for steel 10Kh9V2MFBR after a creep test in regions of the head and of the functional part of a specimen are presented in Fig. 4. The creep test did not cause considerable changes in the structure of packet martensite in the head of the specimen, which consists of troostomartensite just like after tempering. This confirms the fact that neither cell formation nor static recrystallization develop in the steel due to long-term annealing at 650°C. Only plastic deformation can change the structure of steel 10Kh9V2MFBR at this temperature.

Close to the place of failure the microstructure of the specimen tested for creep differs qualitatively from the structure after tempering. It can be seen from Fig. 4*b* that it consists of equiaxed grains/subgrains with uneven boundaries. Despite the considerable difference in the microstructures in

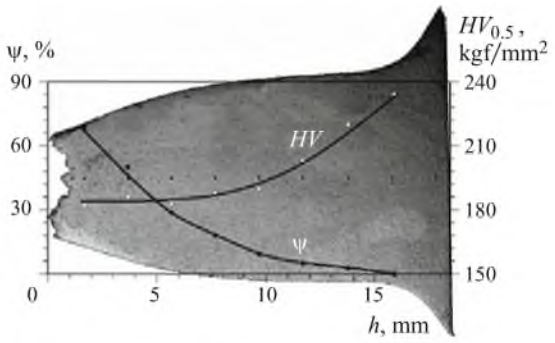

Fig. 3. Variation of the hardness and contraction in a specimen of refractory steel 10Kh9V2MFBR after testing for creep at 650°C (h is the distance from the fracture).

the head and in the neck of the specimen the distribution of the grain/subgrain boundaries with respect to the angles of off-orientation is about the same in both regions. The distributions of the off-orientations are characterized by two peaks corresponding to the small-angle boundaries ($\theta < 15°$) and the large-angle boundaries ($\theta \approx 60°$). The small difference in the distributions of the boundaries/subboundaries off-orientations in the region of the neck consists in the lower fraction of the boundaries with off-orientation of 60°; this reflects the decrease in the specific fraction of the $\Sigma 3$ special boundaries, which is equal to about 7 and 3% in the head and in the neck of the specimen, respectively.

A typical fine structure in a specimen tested for creep is presented in Fig. 5. In the head of the specimen the dislocation substructure of packet martensite remains virtually unchanged after the creep test. The transverse size of the laths is still 330 nm as in the initial tempered state, and the dislocation density inside the packets decreases inconsiderably to 4.4×10^{14} m^{-2}. However, in the neck of the specimen the initial substructure of packet martensite has transformed fully into an equiaxed subgrain structure (Fig. 5*b*). Such structure is typical for hot treatment of materials with high energy of stacking defects, when the evolution of the microstructure occurs by the mechanism of dynamic cell formation. The transverse size of the subgrains is 740 nm, and the dislocation density inside the subgrains has decreased to about 10^{14} m^{-2}.

The effect of the creep on the size distribution of particles of secondary phases that have been located primarily over boundaries of blocks and packets after the tempering is presented in Fig. 6. The size distribution of particles in the initial tempered state is characterized by a narrow range (from 20 to 170 nm). After the creep test this sharp maximum decreases and widens toward larger values, especially in the neck of the specimen. In the head the mean size of the particles of secondary phases increases to 112 nm, whereas in the neck of the specimen the sizes of the particles of secondary phases vary from 60 nm to about 500 nm with a mean size of about 211 nm. The results of an element analysis of

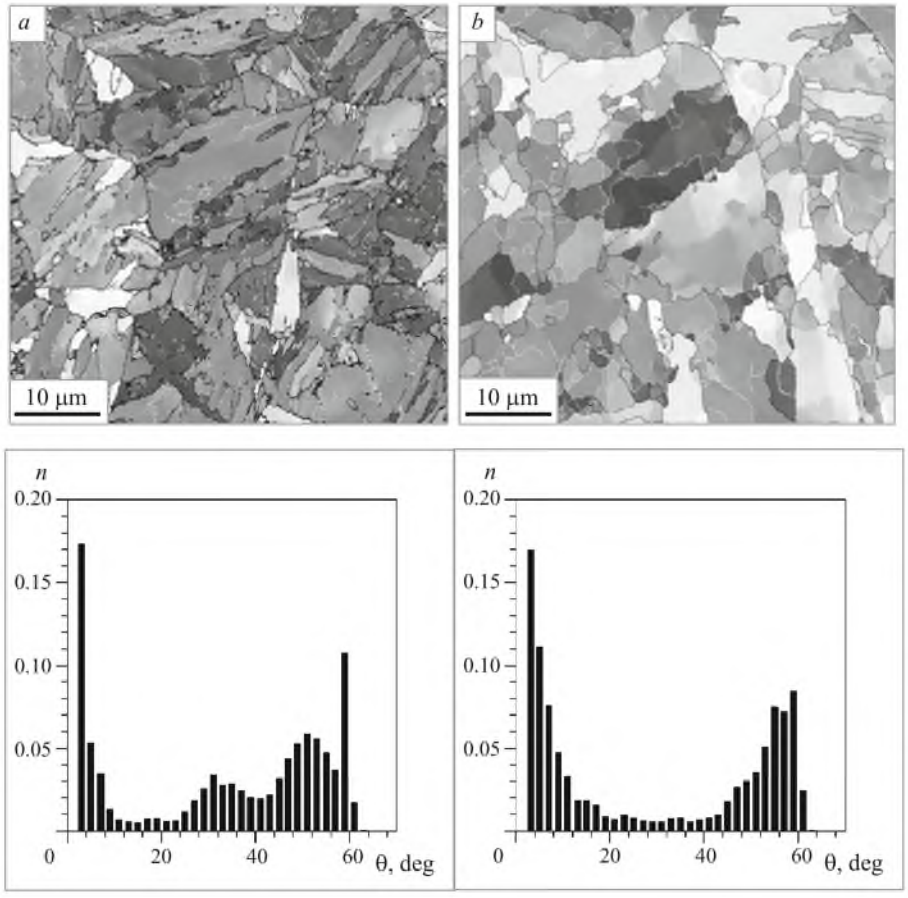

Fig. 4. Maps of off-orientations and distribution of grain/subgrain boundaries with respect to the off-orientation angles in the head (*a*) and in the neck (*b*) of a specimen of steel 10Kh9V2MFBR after creep testing at 650°C (*n* is the numerical fraction of the boundaries and θ is the off-orientation angle). The boundaries with off-orientation less than and greater than 15° are shown white and black respectively.

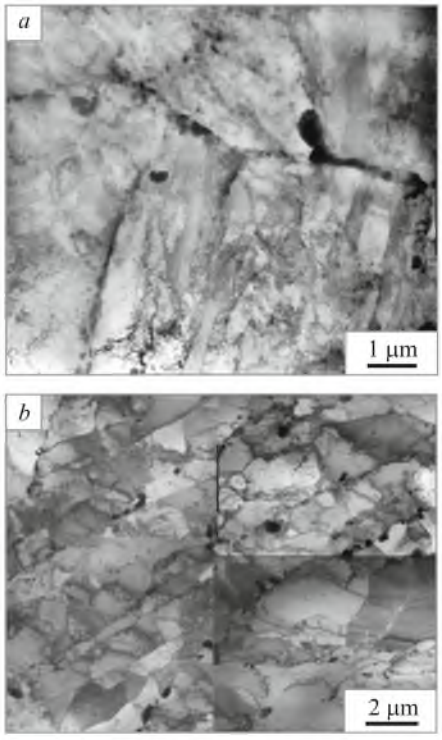

Fig. 5. Substructure in the head (*a*) and in the neck (*b*) of a specimen of steel 10Kh9V2MFBR after testing for creep at 650°C.

individual particles show that the Laves phases coarsen more rapidly than the carbides (Fig. 7), which matches the data of [4, 6 – 9]. Growth in the size of the particles of secondary phases lowers the effect of stabilization of the troostomartensite structure. It can be seen from Fig. 7 that the comparatively larger particles of the $Me_{23}C_6$ carbides and Laves phases are preserved inside the large subgrains formed in the region of the neck. It should also be noted that the size of the subgrains exceeds substantially the thickness of the martensite crystals in the head after annealing. The boundaries of former martensite crystals migrate and this causes decrease in the density of the lattice dislocations accompanied by rearrangement of dislocations inside the small-angle boundaries of these crystals. The latter fact causes decrease and even a complete disappearance of the active stress fields from these boundaries (see Fig. 5*b*). For this reason the small-angle boundaries of the martensite crystals become subgrain boundaries. Migration of dislocation boundaries of former martensite crystals becomes possible as a result of coagulation of V(C, N) particles that hinder this migration. Only spherical carbonitrides with a mean size of about 30 nm are observed inside subgrains after creep tests (Fig. 8). Me(C, N) carbonitrides with a size below 10 nm have not been detected inside the matrix despite the use of special TEM techniques.

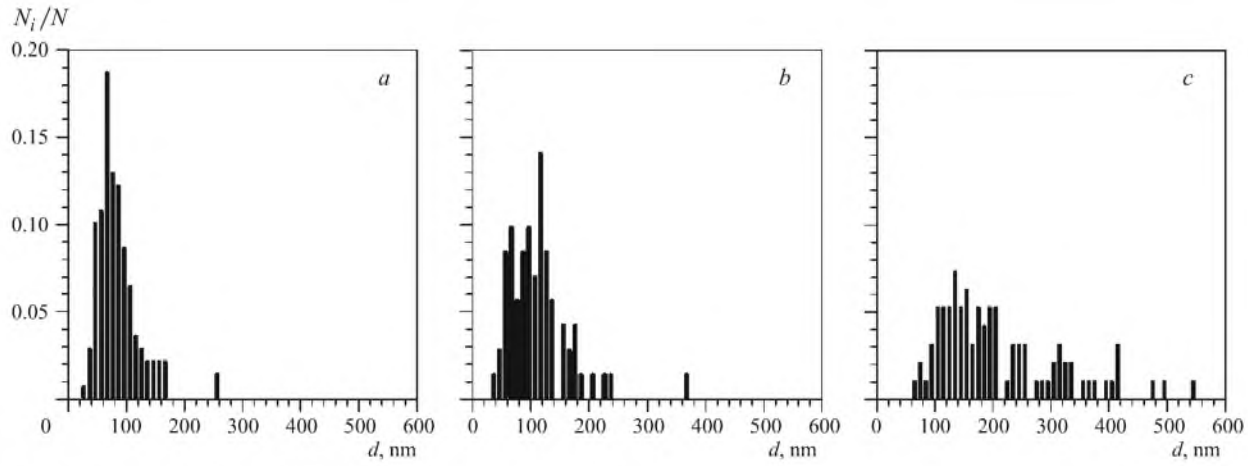

Fig. 6. Size distribution of particles of secondary phases segregated over boundaries of blocks and laths in refractory steel 10Kh9V2MFBR (N_i is the number of particles matching the specified size range, N is the total number of particles): *a*) tempered martensite, d_m = 85 nm; *b*) after testing for creep (the head of the specimen), d_m = 112 nm; *c*) after testing for creep (the neck of the specimen), d_m = 211 nm.

DISCUSSION

The results obtained show that the main process of structural change in steel 10Kh9V2MFBR during creep at elevated temperature is transformation of the small-angle boundaries of former martensite crystals into subgrain boundaries and their migration. The intensity of the migration and, accordingly, the size of the subgrains after creep, are determined by the coagulation of the Me(C, N) carbonitrides, $Me_{23}C_6$ carbides, and Laves phases, which lowers the force hindering the migration of the boundaries. It should be noted that the segregation and growth of the Fe_2W Laves phases causes a decrease in the concentration of tungsten in the solid solution. This has a negative effect on the stability of the dislocation structure of the troostomartensite on the whole due to the growth in the rate of dislocation creep. The changes in the structure of steel 10Kh9V2MFBR depend strongly on the degree of plastic deformation. Let us consider these process during creep in greater detail.

The grain size (D) in metallic materials of matrix type depends on the size (d) and on the volume fraction (F) of the fine particles in accordance with the well known Zener effect of deceleration, i.e., $D = Kd/F$, where F is a factor equal to 0.66 for grains [10]. The functional dependence of the subgrains on the size and specific volume of the fine particles differs from the dependence mentioned only in the value of factor K despite the fact that the mechanisms of the deceleration of migration of small-angle and large-angle boundaries differ markedly [1]. As we have shown above, the dominant boundaries in the former martensitic structure are small-angle ones. The fraction of the special large-angle boundaries is low. For this reason D will be chosen as the size of the subgrains under the additional assumption that at the moment when creep starts it is equal to the width of the martensite crystals.

Segregation of particles of second phases over boundaries of blocks and laths ensures stability of the tempered

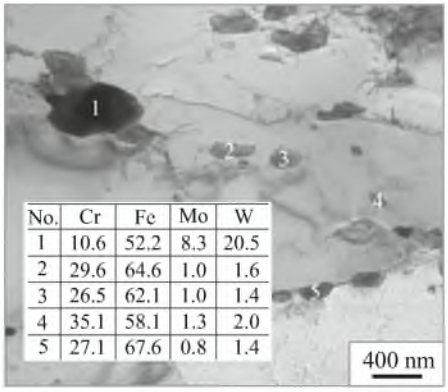

No.	Cr	Fe	Mo	W
1	10.6	52.2	8.3	20.5
2	29.6	64.6	1.0	1.6
3	26.5	62.1	1.0	1.4
4	35.1	58.1	1.3	2.0
5	27.1	67.6	0.8	1.4

Fig. 7. TEM image: $M_{23}C_6$ carbides and Laves phases on boundaries of grains and subgrains in the neck of a specimen of steel 10Kh9V2MFBR after creep tests at 650°C.

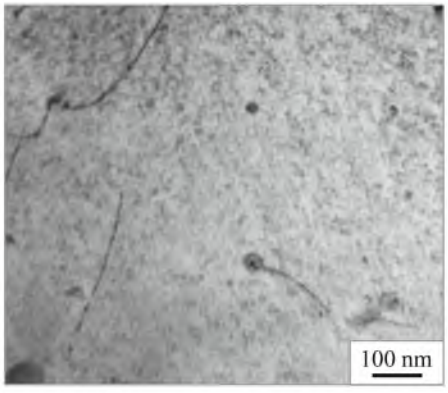

Fig. 8. Fine carbonitrides inside subgrains in the neck of a specimens of steel 10Kh9V2MFBR after testing for creep at 650°C.

martensitic structure at elevated temperatures. Some coarsening of the particles in the head of the specimen under long-term annealing does not cause growth in the sizes of martensite packets. At the same time, the comparatively high plastic deformation ($\varepsilon > 60\%$) in the neck of the specimen is accompanied by coarsening of both particles of secondary phases and martensite packets. In addition, the structure of the martensite loses the initial morphology and is replaced by coarse subgrains formed in the deformation process. It should be noted that the growth in the size of subgrains in the neck of the specimen is almost directly proportional to the growth in the size of the particles. More than doubling of the size of the subgrains correlates with the same growth in the size of the secondary phases. This means that the size of the martensite packets that transform into subgrains in creep obeys the mentioned dependence with $K = 3$, which agrees with the data of numerous studies [12, 13] that predict variation of K from 0.16 to 0.33.

Transformation of the dislocation structure of troostomartensite into a subgrain structure results in softening of the steel. Another cause of softening in creep is growth in the sizes of fine carbonitrides inside the martensite crystals. Increase in the size of the particles of V(C, N) from 6 nm (diameter of an equivalent sphere) in tempered martensite to 30 nm in the place of the neck after testing the specimen for creep increases the distance between the closest particles of Me(C, N) from 100 to 430 nm. This corresponds to decrease in the Orowan stress by $\Delta\tau_O \approx 140$ MPa or $\Delta\sigma_O \approx 280$ MPa. The latter value is close to the difference in the strength values of the tempered specimen and of the neck after testing the specimen for creep, which amounts to about 290 MPa if we take $\sigma \approx HV/3$ [14]. Consequently, it is the coagulation of the carbonitrides that is primarily responsible for the decrease in the microhardness of the steel at room temperature.

The difference in the size distribution of secondary phases in the head and in the functional part of the specimen shows that plastic yielding accelerates substantially the coarsening of particles of the secondary phases for several reasons [15]. The motion of dislocations leads to a loss in the coherence of the phase boundaries of the carbonitrides, which causes their intense coagulation in the creep process. It can be assumed that the acceleration of the coagulation of the $Me_{23}C_6$-type carbides is connected with tube diffusion of carbon and chromium over dislocations [15]. The $Me_{23}C_6$ carbides and the Fe_2W Laves phases are chiefly located over small-angle and large-angle boundaries (see Fig. 6). Acceleration of tube diffusion over the small-angle boundaries can be connected with growth in their off-orientations and, accordingly, with increase in the dislocation density inside them in accordance with the off-orientation θ of the small-angle boundary and the dislocation density ρ in it, i.e., $\theta = \rho b$, where b is the modulus of the Burgers vector. These particles seem to grow on the small-angle boundaries, the off-orientation of which has increased due to creep. Accordingly, the $Me_{23}C_6$ carbides and the Fe_2W Laves phases lying over the small-angle boundaries with lower off-orientation dissolve. Analysis of the size and volume fraction of these particles lying over the former boundaries of austenite grains both in the head and in the functional part of the specimen shows no substantial difference. This means that the grain boundary diffusion accelerates the coagulation of these particles located over large-angle boundaries similarly in static annealing and in creep.

Simultaneously, the process of dynamic cell formation leads to a decrease in the density of lattice dislocations. It seems that capture of immobile lattice dislocations by migrating small-angle boundaries and arrival of mobile lattice dislocations in them are the main processes responsible for the decrease in the density of the lattice dislocations in creep, which also makes a contribution to the softening of the metal. Another process causing a decrease in the dislocation density is their mutual annihilation (retrogression). Both the retrogression and the rearrangement of dislocations in small-angle boundaries require dislocation creep. The main alloying element that suppresses the creep of dislocations due to growth in the force of atomic bonding in the lattice and, correspondingly, due to decrease in the diffusion rate is tungsten. Formation of Laves phases with composition Fe_2W is unambiguous evidence of segregation of tungsten from the solid solution. Analysis of the chemical composition of the metallic matrix after creep has shown that the tungsten content in it fluctuates from 1 to 1.3%. Consequently, almost every third tungsten atom present in the metallic matrix after tempering leaves it and forms Laves phases. This leads to growth in the rate of the dislocation creep and thus accelerates the transformation of the dislocation boundaries of the martensite crystals into subgrain boundaries and dynamic retrogression in the process of creep.

Two processes develop on the small-angle boundaries during creep, namely, rearrangement of dislocations in the dislocation boundaries of packets of the troostomartensite, which decreases their long-acting stress fields to almost complete disappearance, and decrease in the content and growth in the size of $Me_{23}C_6$ carbides and Fe_2W Laves phases on the small-angle boundaries with enlarged off-orientation angles. As a result, the mobility of the dislocation subboundaries increases substantially [10]. The migration of the small-angle boundaries leads to formation of a substructure of hot deformation. This evolution resembles the process of formation of a three-dimensional net of subgrain boundaries or dynamic cell formation, which occurs in plastic deformation of metallic materials with a high energy of stacking faults [11]. A special feature of the process in steel 10Kh9V2MFBR is the fact that the subgrains form from packets of martensite crystals. This mechanism of evolution of the microstructure can be treated as dynamic cell formation, which is responsible for the softening of steel 10Kh9V2MFBR in creep. Alloying aimed at increasing the creep resistance of this steel should primarily ensure suppression or at least deceleration of the process of dynamic cell formation in creep.

CONCLUSIONS

1. The changes in the structure of steel 10Kh9V2MFBR after 1271-h testing for creep at 650°C depend substantially on the degree of the plastic deformation. The initial structure of tempered martensite in the neck of the specimen with transverse size of the martensite crystals equal to 330 nm transforms into a subgrain structure with a mean size of the subgrains equal to about 740 nm. On the contrary, the microstructure of the troostomartensite in the head of the specimen changes little during aging.

2. Growth of the $Me_{23}C_6$ carbides, segregation and growth of the Fe_2W Laves phases over boundaries of blocks and packets, and coagulation of carbonitrides of type V(C, N) in the volume of the steel lead to coarsening of the subgrains in the functional part of the specimen subjected to creep testing. The mean size of the particles in the testing processes increases from 85 to 211 nm.

3. The mechanism of evolution of the microstructure of the functional part of the specimen during creep can be treated as dynamic cell formation, the development of which causes softening of the material.

This work has been performed with financial support of the Federal Agency for Science and Innovations, Grant No. 02.523.12.3019. The authors are grateful to the Collective Use Center "Diagnostics of the Structure and Properties of Materials" of the Belgorod State University for supplying them with the equipment for structure studies.

REFERENCES

1. R. Vismanathan, J. F. Henry, J. Tanzosh, and G. U. S. Stanko, "Program on materials technology for ultra-supercritical coal power plants," *J. Mater. Eng. Perform.*, **14**(3), 281 – 292 (2005).
2. J. C. Vaillant, Vandenberghe, B. Hahn, and H. Heuser, "T/P23, 24, 911 and 92: new grades for advanced coal-fired power plants – properties and experience," *Int. J. Press. Vess. Piping*, 85, 38 – 46 (2008).
3. F. Abe, "Alloy design of creep and oxidation resistant 9Cr steels for thick section boiler components operating at 650°C," in: *Proc. 4th Int. Conf. Advances in Materials Technology for Fossil Power Plants*, USA (2004), pp. 202 – 216.
4. R. O. Kaibyshev, V. N. Skorobogatykh, and I. A. Shchenkova, "New steels of martensitic class for heat power industry. High-temperature properties," *Fiz. Met. Metalloved.*, **109**(2), 200 – 215 (2010).
5. M. Taneike, F. Abe, and K. Sawada, "Creep-strengthening of steel at high temperatures using nano-sized carbonitride dispersions," *Nature*, **424**, 294 – 296 (2003).
6. J. Hald, "Microstructure and long-term creep properties of 9 – 12% Cr steels," *Int. J. Press. Vess. Piping*, **85**, 30 – 37 (2008).
7. K. Sawada, M. Takeda, K. Maruyama, R. Ishii, M. Yamada, Y. Nagae, and R. Komine, "Effect of W on recovery of lath structure during creep of high chromium martensitic steels," *Mater. Sci. Eng. A*, **A267**, 19 – 25 (1999).
8. F. Abe, "Coarsening behavior of lath and its effect on creep rates in tempered martensitic 9Cr – W steels," *Mater. Sci. Eng. A*, **387 – 389**, 565 – 569 (2004).
9. M. Taneike, K. Sawada, and F. Abe, "Effect of carbon concentration on precipitation behavior of $M_{23}C_6$ carbides and MX carbonitrides in martensitic 9Cr steel during heat treatment," *Metall. Mater. Trans. A*, **35A**, 1255 – 1262 (2004).
10. V. A. Dudko, R. O. Kaibyshev, and A. N. Belyakov, "Plastic flow of alloy Fe – 0.6% O obtained by mechanical alloying at a temperature of 550 – 700°C," *Fiz. Met. Metalloved.*, **107**(5), 554 – 560 (2009).
11. F. J. Humphreys and M. Hatherly, *Recrystallization and Related Annealing Phenomena*, Pergamon Press, Oxford (1996), pp. 235 – 279.
12. T. Gladman, "On the theory of the effect of precipitate particles on grain growth in metals," *Pros. R. Soc. London A*, **294**, 298 – 309 (1966).
13. A. K. Koul and F. B. Pickering, "Grain coarsening in the Fe – Ni – Cr alloys and the influence of second phase particles," *Acta Metall.*, **30**, 1303 – 1308 (1982).
14. A. Belyakov, Y. Sakai, T. Hara, et al., "Effect of dispersed particles on microstructure evolved in iron under mechanical milling followed by consolidating rolling," *Metall. Mater. Trans.*, **32A**, 1769 – 1776 (2001).
15. S. Z. Bokshtein, *Structure and Properties of Metallic Alloys* [in Russian], Metallurgiya, Moscow (1971).